

## Magnetic Steel Health Monitoring in the Nano-Scale

Angeliki Mpaliou<sup>1</sup>, Tatiana Damatopoulou<sup>1</sup>, Spyros Angelopoulos<sup>1</sup>, Petros Tsakiridis<sup>1</sup>, Gregory Doumenis<sup>2</sup>, and Evangelos Hristoforou<sup>1</sup>

<sup>1</sup>Laboratory of Electronic Sensors, National Technical University of Athens, Zografou Campus, Athens 15780, Greece

<sup>2</sup> Department of Informatics and Telecommunications, University of Ioannina, Ioannina 47150, Greece  
e-mail: damatat5@yahoo.gr

**Abstract**— In this paper, we demonstrate the first trial to perform steel health monitoring inside the steel grain, by comparing the misorientation of the Kikuchi lines with magnetic properties, namely the Barkhausen noise (BHN), differential magnetic permeability and coercivity. The results illustrate monotonic dependence on the magnetic properties on the crystalline misorientation. Apart from that, microhardness studies have also been realized, illustrating a monotonic dependence on magnetic properties. Such monotonic dependence allows for the correlation of magnetic properties on mechanical properties and residual stresses and their corresponding use for industrial applications towards steel health monitoring.

**Keywords:** Residual stresses; electron back scattering; Barkhausen noise; magnetization loop.

### I. INTRODUCTION

Magnetization process is evidently dependent on the structure and microstructure of the magnetic substance [1]. The presence of dislocations and nano-precipitates affects both magnetic domain wall mobility and magnetic domain rotation [2]. Thus, magnetic properties, such as M-H loops, Barkhausen noise (BHN), the Magneto-Acoustic Emission (MAE) and the surface magnetic permeability of steels are dependent on the presence of sub-grains, plastic deformation and the size & distribution of nano-precipitates in the grain: they are the reason of residual stresses and mechanical properties, such as hardness and microhardness [3]. The dependence of the magnetic properties on the microstructure is modeled with respect to the dependence of domain wall motion and domain rotation on dislocations and nano-precipitates [4].

We have worked for a long time to develop methodologies and technology to determine residual stresses in the mesoscopic level. This has been achieved by considering residual stresses as an average among a number of grains in ferrous steels [5]. Such analysis has contributed to the quality control of production lines related to steel production and manufacturing, as well as to steel end users. Therefore, it allowed for the actual determination of the distribution of the residual stress tensor on the surface and in the bulk of the ferromagnetic steel [6].

However, the technology up to now has been limited to an average minimum volume of stress detection in the order of  $10 \text{ cm}^3$  [7]. The motivation of the current work has been

the initiation of studies related to the correlation between magnetic properties and misalignment of the crystalline structure within the grains of magnetic steels. Such a correlation may result in indirect determination of microstrain distribution, anisotropy change and localized microhardness determination within the steel grain.

The materials and methods used are described in Chapter II, followed by experimental analysis using Electron Back Scattering Diffraction (EBSD) studies (Chapter III). Then, a new type of sensor is proposed to precisely monitor residual stresses in minimized surfaces (Chapter IV). Finally, a new method for generating residual stresses in a steel coupon is discussed, offering significant advances in the amplitude of the developed residual stresses in the steel samples (Chapter V).

### II. MATERIALS AND METHODS

Armco steel, with less than 7 ppm carbon and 5 ppm sulfur, has been chosen as the type of steel to initiate this type of measurements, due to its single phase ferritic structure, similar to the electric steel structure. Armco steel samples have been cold-rolled up to 65% reduction of cross section and then they have been properly polished to undergo EBSD, using Struers polishing instrumentation [8]. EBSD studies were realized using a JEOL 6380LV scanning electron microscope, equipped with a Thermo Fisher Scientific EBSD instrumentation to determine the misalignment of Kikuchi lines inside the grains and therefore to determine the degree of misorientation of the crystalline structure in the grains of the Armco steel. The polished Armco samples, as well as Armco samples directly after cold rolling, have been used to determine their magnetic properties. Two different magnetic measurements have been realized, namely Barkhausen noise (BHN) [9], as well as M-H hysteresis loop measurements [10]. The BHN measurements were realized by the MEB 2c instrument from Mag-Lab sc; Gdansk, Poland [11]. M-H loop measurements were realized by a home-made set-up employing a Kethley signal generator, a KEPCO current amplifier, an MFLI Lock-in Amplifier, and an Agilent 200 MHz oscilloscope. BHN measurements offered the local number of Barkhausen jumps and the BHN envelope, while the M-H loops offered the local coercivity  $H_c$  and remanence  $M_R$ , at the region of measurements.

Finally, microhardness measurements have been realized using the facilities of the Research and Standardization Centre of the Power Public Corporation of Greece.

### III. EXPERIMENTAL RESULTS

The grain misorientation is illustrated by means of pole figures of EBSD (Figure 1), following the Thermo Fischer Scientific calculations based on the Kikuchi lines determination in sub-micron regions. Misorientation was found to be enhanced with respect to cold rolling process, as expected. The dependence of misorientation angle of the grains on the cold rolling reduction is illustrated in Figure 2. Apart from that, misorientation angle was also correlated with microhardness of the cold rolled Armco steel, as illustrated in Figure 3. Following the EBSD characterization, BHN measurements were realized, by means of mapping the whole surface of the Armco steel. Figure 4 illustrates a typical response of BHN mapping under different reduction percentages.

The correlation between BHN measurements was realized with respect to microhardness measurements: BHN envelop and microhardness dependence on cross section reduction is illustrated in Figure 5. The systematic monotonic tendency can be seen, with a rather large uncertainty, due to the mismatching in the pointed microhardness and BHN measurements. The correlation between magnetic properties determined by the M-H loop illustrates significantly better uncertainty, due to the more averaging nature of the method. A typical dependence of the coercive field on the EBSD-determined misorientation angle is illustrated in Figure 6.

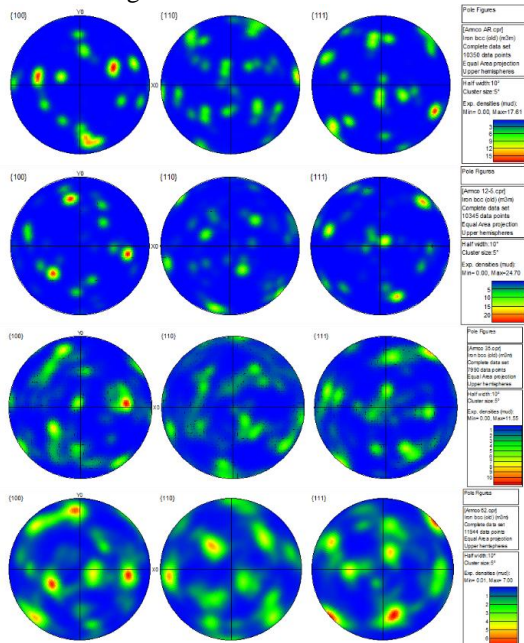


Figure 1. Pole figures of the cold rolled Armco steel samples. From top to bottom: 25%, 12,5%, 50%, 62,5% cross section reduction, illustrating an increase of misorientation with cross section decrease.

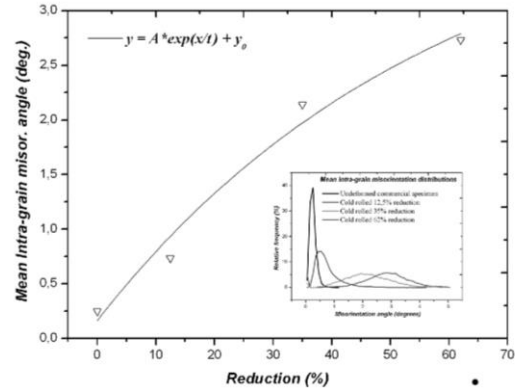


Figure 2. Dependence of the misorientation angle on the reduction % of the Armco steel.

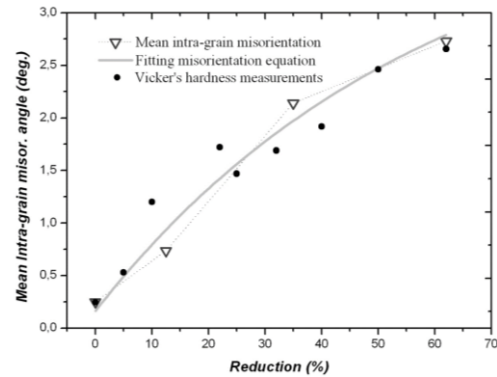


Figure 3. Comparison of the mean intra-grain misorientation angle and the Vicker's hardness in different cross section reduction.

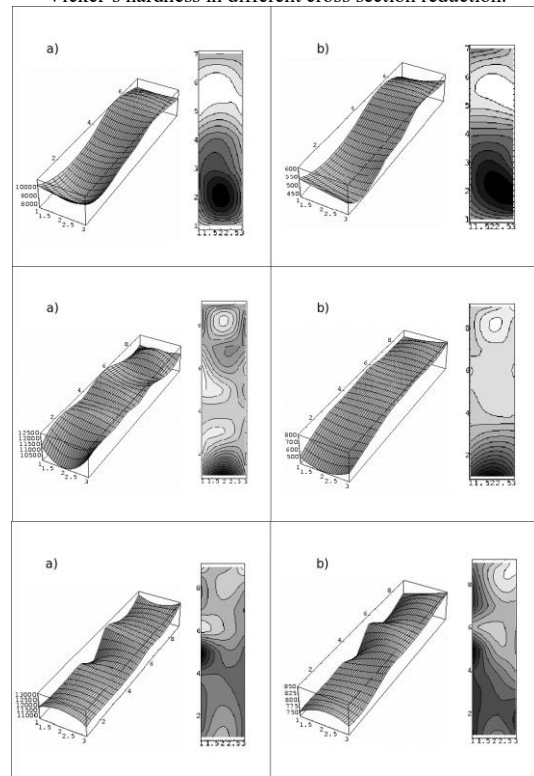


Figure 4. BHN mapping on the surface of cold rolled Armco steel. BHN counts are represented in (a) and BHN envelop is represented in (b). Top: 25% cold rolling. Middle: 50% cold rolling. Bottom: 62,5% cold rolling.

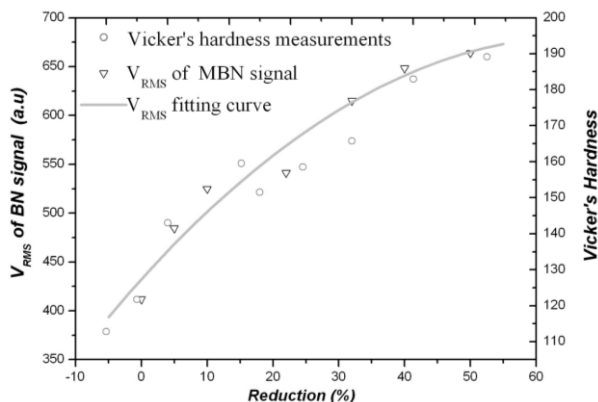


Figure 5. Dependence of BHN envelope and microhardness on the cross section reduction of the Armco steel.

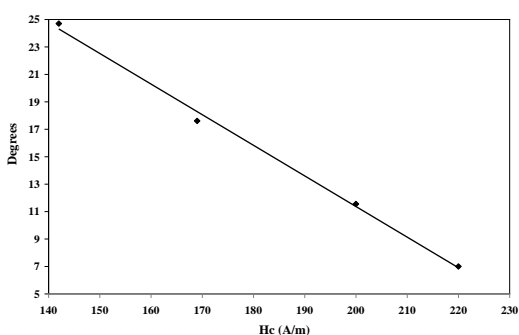


Figure 6. Typical dependence of the crystalline misorientation angle in a sum of grains in the Armco steel on the average coercive field in the same area.

Furthermore, the dependence of the remanence magnetization  $M_R$  on the microhardness of the Armco steel samples is illustrated in Figure 7. A clear monotonic dependence with lower uncertainty is observable. Magnetic measurements of the cold rolled Armco steel were realized not only after polishing the cold rolled samples, but also directly after cross section reduction, illustrating almost the same behavior. This means that the surface roughness of the cold rolled samples is not an issue for hard measurements, this allowing for easier industrial use of the method.

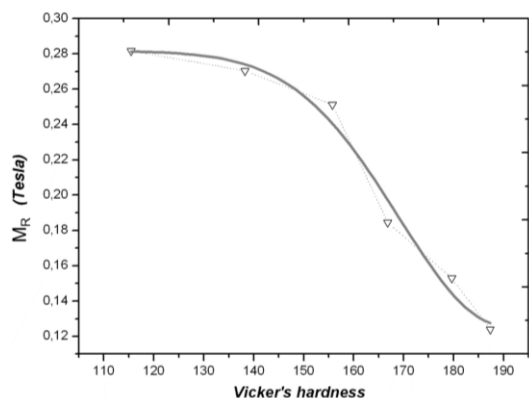


Figure 7. Dependence of the remanence magnetization  $M_R$  on the Vicker's hardness.

A similar type of magnetic measurements, employing the determination of the differential magnetic permeability in different types of steels, including Armco steel, have also been realized, illustrating a similar, or even more sensitive, characterization tool [12]. The above mentioned magnetic techniques can be employed to determine the level of plastic deformation of steels, thus improving the existing state of the art in steel non-destructive testing for the plastic deformation region, offering the possibility of early stage steel structural health monitoring. The most straightforward result from the illustrated experimental results is that the grain misorientation angle of cold rolled ferritic steel samples is monotonically dependent on the cross section reduction and the magnetic properties of the steel.

Furthermore, the application-oriented interesting result is the monotonic dependence of macroscopic magnetic properties on the Armco steel microhardness. The dependence of coercivity and remanence on microhardness is clearly demonstrating the ability of M-H characterization to operate as a microhardness determination tool. Since it is a non-destructive approach, the ease of measurement allows for practical industrial and field application. Bearing in mind the similarity of the Armco steel with electric steels, which have the same microstructure as Armco steel, the methodology and technology presented in this article can be used for the characterization of electric steel, which opens a new era in faster and non-destructive characterization of electric steels, with so important applications in our days, namely their use in electric vehicles. This fact is considered as a significant add-on the technology of electric steel (and ferritic steel in general) non-destructive characterization. The thermal stamping of these steels to develop either stators or rotors, results in residual stresses, thus affecting the magnetic permeability and thus the performance of the electric motors. The classical method of annihilating such stresses and corresponding recovery of magnetic properties of these stators and rotors is the heat annealing of the whole stator or rotor. This may result in mechanical softening of the rest of the electric steel, instead of the cutting region only. Using such localized stress measurements, stress annihilation and therefore permeability optimization can be realized, only in the region of elevated residual stresses, using localized RF induction heating at ranges of excitation current, corresponding to the level of residual stresses.

However, these are the first results of magnetic steel structural health monitoring in the nanoscale, related to a single phase magnetic steel. In order to actually evaluate the ability of magnetic measurements to offer monotonic dependence on multiphase ferromagnetic steels, including low carbon steels (carbides), austenitic steels suffering martensitic transformation, dual or multi-phase steels like Duplex steels, or even high entropy alloys demonstrating magnetic properties, a systematic work on such characterization is required. Such work must be realized

most probably in an inter-laboratory comparison procedure, since it is important for the steel industry in total: it reduces the cost and the time for quality control of the under test steel, permitting total quality control in all steel production and manufacturing due to its non-destructive character. But all magnetic measurements presented in this work, even the BHN measurements refer to at least a  $\text{mm}^2$  surface measurement, thus averaging a vast number of grains in terms of magnetic measurements. Therefore, a magnetic method to provide magnetic measurements with the same spatial resolution is needed, to take full advantage of the method. The existing state of the art in such technology is the magnetic force microscopy (MFM), allowing for a very similar spatial resolution in comparison to the EBSD method [13]. Of course, the MFM technology cannot be industrially used. For this reason, an industrially applicable method and technology is required to achieve measurements with a spatial resolution in the order of micrometers. Such a sensor is presented in the next session of this work.

#### IV. A MICRO SIZED PERMEABILITY SENSOR

The principle of such a microsensor is depicted in Figure 8. The sensor offers spatial resolution in the order of  $\mu\text{m}$ , with a sampling rate in the order of  $\mu\text{s}$  [14]. Pulsed current is transmitted to the thin film pulsed current conductor, which splits into two thin film pulsed current conductors of the same dimensions, thus being able to transmit the same amount of current through them. A thin film magnetic field layer is set between the two pulsed current conductors, able to monitor magnetic field along its surface. Two insulating thin films are used to separate the thin magnetic film from the two thin film pulsed current conductors. The external side of the thin film pulsed current conductor accommodates the sensor electronics, including its stored calibration data, preferably in the form of application-specific-integrated-circuit (ASIC). The external side of the thin film pulsed current conductor accommodates the thin film external packaging of the sensor, which can attach the surface of the ferromagnetic steel under measurement.

An electronic circuit, preferably embedded in the sensor and the mentioned ASIC is used to wirelessly transfer the data of the sensor. A position sensor, indicatively being a photonic sensor, like those operating in the mouse of a personal computer, or even an interferometer, is used for monitoring the position of the magnetic thin film, the output of which is connected to the electronic circuit, thus wirelessly transferring the position data of the sensor. The operation of the sensor is as follows: the thin film external packaging of the sensor touches the surface under measurement and the output of the thin magnetic film is monotonically dependent on the surface permeability and the residual stresses of the surface area of the steel under measurement, defined by the projection of the surface of the thin magnetic film. These data in the form of stress components and positions are transmitted to a portable computer or tablet or smartphone, offering the mapping of

the surface stress tensor distribution by using the in-house application-specific-software.

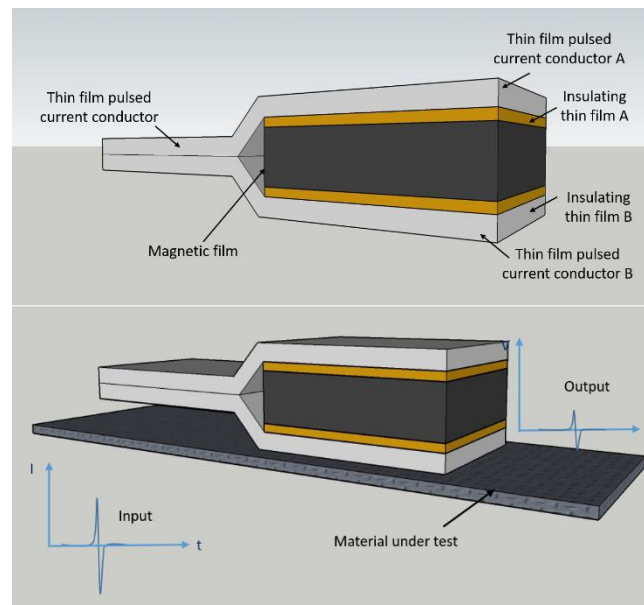


Figure 8. The new microsensor for surface permeability measurements (top) and its operation (bottom)

When pulsed current is transmitted through the two pulsed current conductors, they generate magnetic field parallel to their surface, which penetrates the thin film magnetic sensor. The fields  $H_1$  and  $H_2$  from the two pulsed current conductors are proportional to the transmitted pulsed currents  $I_1$  &  $I_2$  to each one of them, and inversely proportional to the distance  $d_1$  &  $d_2$  between the said pulsed current conductors and the thin magnetic film:

$$H_1 = a \frac{I_1}{d_1} \quad (1)$$

And

$$H_2 = -a \frac{I_2}{d_2} \quad (2)$$

Where  $a$ , is a proportionality constant. Considering the pulsed currents  $I_1$  &  $I_2$  equal each other and the distances  $d_1$  &  $d_2$  equal each other then, the total field  $H$  along the surface of the thin magnetic film is:

$$H = H_1 + H_2 = a \frac{I}{d} + \left(-a \frac{I}{d}\right) = 0 \quad (3)$$

Thus, the output of the thin film sensor equals zero and corresponds to its zero reference field.

When the sensor, and particularly the packaging part of it approaches the ferromagnetic steel under measurement, provided that the distance between the packaging part of the sensor and the ferromagnetic steel is small (in the order of a few  $\mu\text{m}$ ), the magnetic lines due to the field  $H_1$  are partially trapped by the ferromagnetic steel under measurement, allowing only a part of the magnetic field  $H_1$  to remain in the volume of the thin magnetic film:

$$H_1 = H_1 - H_1^\mu \quad (4)$$

Where  $H_1^\mu$  is the magnetic field corresponding to the magnetic lines trapped by the surface of the ferromagnetic steel under measurement, which are dependent on the



surface permeability of it. Instead, most of the magnetic lines due to the field  $H_2$  remain in the area close to the thin magnetic film according to Maxwell equations. Therefore, an imbalance in the magnetic field within the volume of the thin magnetic film is generated and  $H$  becomes:

$$H = -H_1^{\mu} \quad (5)$$

Therefore, the output of the thin magnetic film is proportional to the surface permeability component of the ferromagnetic steel under measurement, parallel to the magnetic fields  $H_1$  &  $H_2$ . It is also known that the permeability component  $\mu$  of a ferromagnetic steel is proportional to the residual stress component  $\sigma$  in the area of its surface and the corresponding direction or in a corresponding volume just below it:

$$\sigma = b\mu \text{ or } \sigma_x = b\mu_x \text{ \& } \sigma_y = b\mu_y \quad (6)$$

Therefore, the output of the thin magnetic film is proportional to the stress component parallel to the magnetic fields  $H_1$  &  $H_2$ . Change of orientation of the sensor or manufacturing of several sensors in the same chip, in corresponding directions, offers the ability of monitoring the stress components on the surface of the ferromagnetic steel under measurement. The thin magnetic film can be in any of the existing, industrially available thin magnetic film field sensors, namely anisotropic magnetoresistance (AMR) sensors, giant magnetoresistive (GMR) sensors, spin valve sensors, etc. The largest surface of these sensors, currently available in the market of ASIC, like permalloy films, is far below  $100 \mu\text{m} \times 100 \mu\text{m}$ , while the surface of  $1 \mu\text{m} \times 1 \mu\text{m}$  thin film magnetic field sensor is easily achievable in the form of AMR arrangement following classical microelectronics technology. Thus, the special resolution of the sensor can easily be in the order of  $1 \mu\text{m}^2$ . Apart from that the excitation and the reading ability of electronics can be less than  $1 \mu\text{s}$ , thus allowing for single point measurements in less than 1 point per  $1 \mu\text{s}$ . The sensitivity and uncertainty of the stress sensor are dependent on the sensitivity and uncertainty of the implemented thin film magnetic field sensor. Bearing in mind that the worst sensitivity of the above mentioned thin film magnetic field sensors (AMR, GMR etc.) is  $1 \text{ nT} @ \text{Hz}^{-1/2}$ , the sensitivity of the sensor in pulsed operation is better than  $1 \text{ nT}$ . Motion of the sensor along the surface of the ferromagnetic steel under measurement, and use of the data from the position sensor offers the dependence of the stress components on the different areas of the surface of the ferromagnetic steel under measurement.

### V. DISCUSSION

This type of magnetic measurement can be realized in electric steel production manufacturing lines. The new era of electric motion requires significantly advanced cores for stators and rotors, thus permitting reduction of size and weight of electric motors. The methodology and technology presented in this paper can be used for microstructural characterization and mechanical properties determination, both being important for the proper quality control of the produced electric steel. Therefore, a robotic system based on

the measuring methods presented in this paper, the total quality control of the whole electric steel production can be realized, thus offering a significant advantage to the electric steel producers following the methodology. Furthermore, the electric steel manufacturers, using hot stamping technology to develop parts of the stator and rotor of electric machines can also use this technology in order to locally annihilate the electric steel at the surfaces of stamping, by using localized induction heating. An example of such treatment is illustrated in Figure 9, where a simple RF heater with point high frequency conductors can be used to locally apply eddy currents and correspondingly generate localized heat in the material. Due to the relatively low thermal conductivity of steels, heat is rather concentrated in the area of eddy currents, allowing for localized stress annihilation process. Experiments have also been realized in oriented and non-oriented electric steel sheets, which have undergone localized heating and consequent quenching (Figure 10). Temperature was elevated up to  $300^\circ\text{C}$  and  $500^\circ\text{C}$  with consequent quenching with water. The quenched areas of the surface of the steel sheets can be seen by naked eye. After quenching, thermal treatment resulted in annihilating residual stresses for the case of  $300^\circ\text{C}$ . However, such annihilation was not achievable for the case of  $500^\circ\text{C}$  heated and consequently quenched electric steel sheet.



Figure 9. RF heater for localized stress annihilation

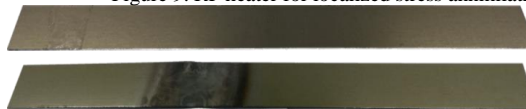


Figure 10. Quenched electric steel after heating in  $300^\circ\text{C}$  and  $500^\circ\text{C}$ . The quenched areas can be seen by naked eye.

The same principle can also be used for determination of the magnetic stress calibration (MASC) curve in steels [6], allowing for the proper development of data for the calibration of residual stress determination of steel sheets. Future work has already been initiated for this purpose, requiring additional inter-laboratory tests to verify the level of uncertainty of measurements. An example of such a MASC based on the RF induction heating and consequent quenching is illustrated in Figure 11, for electric steel and 42CrMo4 steel. These measurements have been determined

using an AMR sensor, with direct correlation of the AMR output in  $\mu\text{T}$  with residual stresses in MPa. Such a response is enhanced with respect to our previous method for the determination of MASC curve, using welded samples, for several reasons, the most important being the maintenance of the steel phase. However, even the use of this technique, named 3MA technique, suffers from the problem of not being able to recon between positive and negative magnetostrictive ematerials. This issue is overcome by using our patented microsensor. The nature of manufacturing this type of sensor allows for the development of two sensors with  $90^\circ$  shift, thus allowing simultaneous measurement of two directions, resulting in the determination of surface permeability in both axes, which may be used for determination of the effective field caused by positive and negative magnetostriction. Results based on this principle are illustrated in Figure 12, where the measurement of localized stresses can be seen for the case of a non-oriented electric steel sheet, heated and water-quenched in  $500^\circ\text{C}$ . Such a response demonstrates the main principle of innovation presented in this paper.

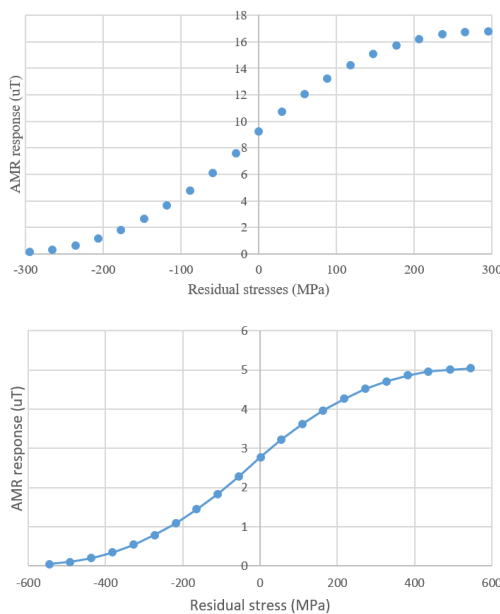


Figure 11. New MASC curves based on the RF induction method. Top: Electric Steel MASC curve. Bottom: 42CrMo4 steel MASC curve.

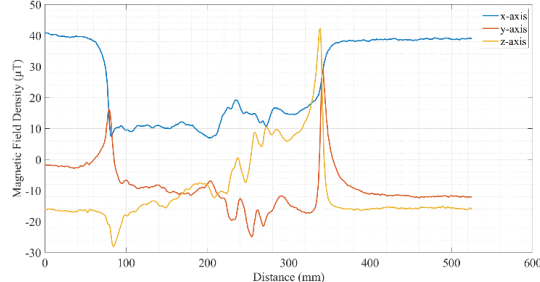


Figure 12. Monitoring residual stresses as a result of quenching in NOES.

## VI. CONCLUSIONS

A non-destructive method for the determination of the micro-structural misorientation in cold rolled Armco ferritic steels has been presented in this article. Apart from that, the presented methodology allows for the determination of hardness in this type of steel. All measurements demonstrate a monotonic dependence of magnetic properties on the misorientation angle and microhardness of plastically deformed samples. A new, patented, type of sensor has also been presented, able to detect surface magnetic permeability with spatial resolution in the order of  $\mu\text{m}^2$ . Finally, a new method for developing residual stresses in steels is also proposed, allowing for easier inter-laboratory comparison tests with better levels of uncertainties. Future work, based on these inter-laboratory tests is required to achieve the initial work for the preparation of a related Standard of residual stress measurements and their correlation with magnetic properties.

## ACKNOWLEDGMENT

This work was supported by the European Union and Greek National Funds through the Operational Program Competitiveness, Entrepreneurship and Innovation, under the call RESEARCH-CREATE-INNOVATE under Project T2EDK-02521.

## REFERENCES

- [1] J. M. D. Coey, "Magnetism and magnetic materials", Cambridge University Press, 2010
- [2] S. Takahashi, J. Echigoya, and Z. Motoki, "Magnetization curves of plastically deformed Fe metals and alloys", *J. Appl. Phys.* 87, 805–813 (2000), <https://doi.org/10.1063/1.371945>
- [3] I. Altpeter, G. Dobmann, M. Kröning, M. Rabung, and S. Szielasko, "Micro-magnetic evaluation of micro residual stresses of the IInd and IIIrd order", *NDT & E International* 42 (4), 283-290, 2009
- [4] E. Olivetti, F. Fiorillo, E. Forton, L. Martino, and L. Rocchino, "Microstructure and magnetic properties of pure iron for cyclotron electromagnets", *Journal of Alloys and Compounds*, 615, Pages S291-S295, 2014
- [5] P. Vourna, A. Ktena, P. Tsakiridis, and E. Hristoforou, "A novel approach of accurately evaluating residual stress and microstructure of welded electrical steels", *NDT and E International* 71, pp. 33-42, 2015
- [6] E. Hristoforou, P. Vourna, A. Ktena, and P. Svec, "On the Universality of the Dependence of Magnetic Parameters on Residual Stresses in Steels", *IEEE Transactions on Magnetics* 52(5),7362189, 2016
- [7] A. Ktena, E. Hristoforou, "Stress dependent magnetization and vector preisach modeling in low carbon steels", *IEEE Transactions on Magnetics* 48 (4), 1433-1436, 2012
- [8] D. J. Dingley, V. Randle, "Microtexture determination by electron back-scatter diffraction". *J Mater Sci.* 27, pp. 4545–4566, 1992
- [9] D. Spasojević, S. Bukvić, S. Milošević, and H. Eugene Stanley, "Barkhausen noise: Elementary signals, power laws, and scaling relations", *Phys. Rev. E.* 54, 2531-2546, 1996

- [10] D. L. Atherton, D. C. Jiles, "Effects of stress on magnetization", *NDT international* 19.1, 15-19, 1986
- [11] L. Piotrowski, B. Augustyniak, M. Chmielewski, E. V. Hristoforou, and K. Kosmas, "Evaluation of Barkhausen Noise and Magnetoacoustic Emission Signals Properties for Plastically Deformed Armco Iron," *IEEE Transactions on Magnetics*, 46, 239-242, 2010
- [12] P. Vourna; E. Hristoforou; A. Ktena; P. Svec; and E. Mangiorou, "Dependence of Magnetic Permeability on Residual Stresses in Welded Steels", *IEEE Transactions on Magnetics*, 53, Article 6200704, 2017
- [13] E. Sarantopoulou, S. Kobe, K. Z. Rozman, Z. Kollia, G. Drazic, and A. C. Cefalas, "Fabrication of magnetic SmFe films by pulsed laser deposition at 157 nm", *IEEE Transactions on Magnetics*, 40, pp. 2943-2945, 2004
- [14] Multi-layer thin film sensor for non-destructive testing of perromagnetic materials, US Patent, 072517INTEFSW10512900, 2017